

# Condensates in aggregation processes with input: a new power law and intermittency

Reya Negi, Rajiv G Pereira, and Mustansir Barma<sup>1</sup>

<sup>1</sup>*TIFR Centre for Interdisciplinary Sciences, Tata Institute of Fundamental Research, Gopanpally, Hyderabad, 500046, India*

Large-mass condensates, which coexist with a power-law-decaying distribution in the one-dimensional Takayasu model of mass aggregation with input, were recently found in numerical simulations. Here we establish the occurrence of condensates by analyzing exact recursions, and further show that they have a strong effect on the properties of the system. In the steady state of a large but finite system, there is a single condensate, whose movement through the system leads to a reorganization of the mass profile on a macroscopic scale. A scaling analysis of the mean mass and standard deviation at different distances from the condensate leads to the surprising conclusion that the mass distribution on sites close to the condensate follow a power-law decay with a new exponent  $5/3$ , while further-away sites show the customary Takayasu exponent  $4/3$ , with a crossover in between. Finally, the exit of condensates from a system with open boundaries has a strong effect on the temporal fluctuations of the total mass in the steady state. Their departure is followed by a build-up of mass and subsequent departures, leading to strong intermittency, established through a divergence of the flatness as the scaled time approaches zero.

Aggregation phenomena are important in many areas of the natural sciences, cutting across different fields and length scales, from clouds and river networks on the one hand, to colloid formation and biomolecular organization on the other [1–7]. The subject, which began with the pioneering studies of colloidal clusters by Smoluchowski [3], continues to find new domains of applicability, most recently in aspects of biomolecular organization [4–7].

The kinetics of aggregation involves the coalescence and breakup of clusters with different numbers of particles, thus different masses. The resulting time-dependent mass distribution often shows interesting features. First, the distribution may be broad, characterized by a power law, signalling scale invariance arising from critical correlations in the system. Secondly, spatially well-separated condensates may form, each one being a single cluster which holds a very large number of constituent particles. It is natural to ask: Under what conditions are these features manifest? Can they arise together, and if so, under what circumstances?

Much can be learned from the analysis of simple models whose definitions include only the essential kinetic processes, but whose emergent behaviour is nontrivial. The Takayasu model of aggregation is a prime example [8–10]. Its moves include diffusion of particle clusters, followed by coalescence when two clusters meet. Further, there is an input of particles at a steady rate. The appeal of the model stems from its simplicity and the fact that as time passes, the distribution of particle numbers approaches a power-law scaling function of mass and time, indicating a self-organized critical (SOC) state. This can be established analytically within mean field theory and through an exact recursive calculation in 1D [8, 9, 11, 12]. In addition, spatiotemporal correlation functions can be calculated exactly [13]. Interestingly, the Takayasu model has exact correspondences to several other models, for instance the Scheidegger model of river basins [2, 13], the voter model [14] and models of

stress propagation in bead packs [15]. Further, experiments indicate that nucleoli in certain living cells share the Takayasu moves of diffusion, coalescence and input, and show a broad power-law distribution of sizes [4–6].

Whereas the power law scaling is well established and known since the inception of the Takayasu model, it is only recently that it was realized that the model also exhibits condensates or extremely large-mass clusters [16]. Condensates are known to arise in aggregation models with mass conservation, where their formation is akin to Bose-Einstein condensation [17–20]. But in the Takayasu model, where the mass is strongly non-conserved owing to the steady input, the mechanism is quite different. It is a purely statistical effect, related to the influence of the largest term drawn from a stable distribution [21–23]. Numerical simulations show that beyond the power law, the probability distribution of masses in the Takayasu model exhibits a strong and distinctive condensate hump, which is part of the scaling function [16], confirmed by the numerically exact recursive results reported below. A time-dependent length scale  $\mathcal{L}(t)$  determines condensate masses and the spacing between them [23]. Since the underlying process is diffusive,  $\mathcal{L}(t)$  is proportional to  $t^{1/2}$ . This implies that as  $t$  increases, the number of condensates falls while the size of each increases, as in phase ordering dynamics [20, 24]. This continues till  $\mathcal{L}(t)$  reaches the system size  $L$ , beyond which a long time state with statistically invariant properties sets in [16].

Condensates have a strong effect on the properties of the Takayasu model. In this paper, we first establish their occurrence by an exact calculation of the probability distribution of mass as a function of time (see Fig. 1c) through recurrence relations of the mass held in a stretch of lattice sites [8, 9, 12]. Further, we investigate the effect of condensates on the mass profile in the system, recognizing that a condensate functions like an efficient forager which ingests mass from neighboring regions. The result is surprising: with periodic boundary conditions,

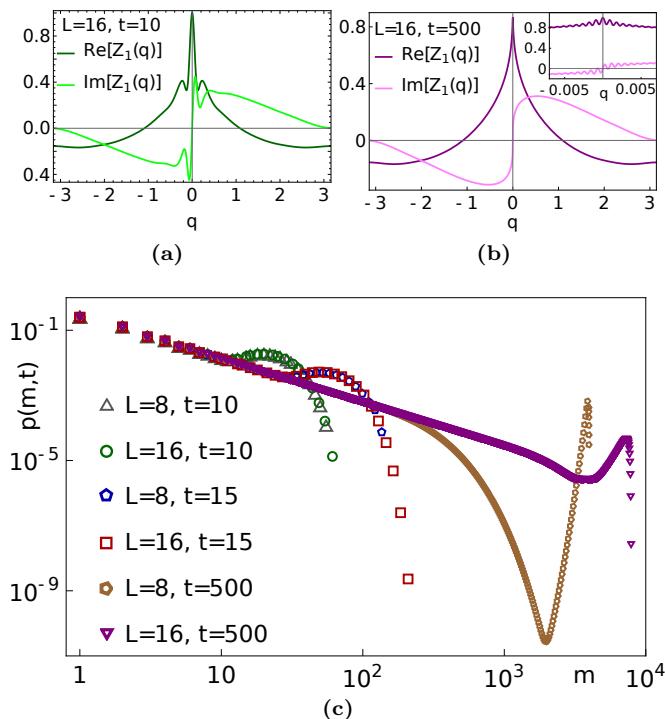


**FIG. 1.** (a), (b) The characteristic function  $Z_1(q, t)$  for  $t = 10 \ll t^*$  and  $t = 500 \gg t^*$  for  $L = 16$ . (c) The probability distribution  $p(m, t)$  for  $L = 8$  and  $16$  in the regimes  $t \ll t^*$  and  $t \gg t^*$ . In the former regime ( $t = 10$  and  $15$ ) the condensates correspond to the hump, while in steady state ( $t = 500$ ), there is a single condensate corresponding to the peak at the right edge.

the mass profile seen by the condensate is reorganized on a *macroscopic* scale. The mean mass profile and its standard deviation are both scaling functions of  $r/L$  where  $r$  is the distance from the condensate. As shown below, the results imply that the distribution of masses on sites close to the condensate follows a new power law  $\sim m^{-5/3}$  as opposed to the well-known Takayasu power  $\sim m^{-4/3}$ , which holds on distant sites. Finally, we investigate the time variation of the mass of a system with free boundary conditions and find that the build-up and departure of condensates leads to enormous fluctuations of the total mass, characterized by strong intermittency, reminiscent of dragon king events [25, 26].

In 1D, the Takayasu model is defined on a lattice with  $L$  sites with site  $i \in \{1, 2, \dots, L\}$  holding a mass  $m(i, t)$ , which is a whole number. We assume periodic boundary conditions so that  $m(i, t) = m(i + L, t)$ . At each time-step the following two steps occur in the system. (1) Diffusion: the entire mass at each site either hops to the neighboring site to the right or stays put with probability  $1/2$ . Note that this can be mapped to the familiar symmetric diffusion of a random walker on moving to a frame which has a velocity  $1/2$  with respect to the lattice [11]. Evidently, the mass distribution is the same in

either description. (2) Input: a unit mass is injected at each site. The dynamics of the system is thus described by the stochastic equation

$$m(i, t + 1) = (1 - W_i(t))m(i, t) + W_{i-1}(t)m(i - 1, t) + 1, \quad (1)$$

where  $W_i(t) = 0$  or  $1$  with probability  $1/2$  each. Our objective is to calculate the probability  $p(m, t)$  to find a mass  $m$  at any site at time  $t$ , given an initial configuration with every site occupied by a unit mass.

Following [11], we consider the mass contained in a stretch of  $r$  consecutive sites at any instant:

$$M_{n,r}(t) = \sum_{i=1}^r m(n + i - 1, t), \quad r = 1, 2, \dots, L. \quad (2)$$

The corresponding probability distribution, which is translationally invariant, has a characteristic function

$$Z_r(q, t) \equiv \langle \exp \{iq M_{nr}(t)\} \rangle, \quad (3)$$

where the average is over all histories. Equations (1) and (2), lead to the recursion relation [11]

$$Z_r(q, t + 1) = \frac{e^{iqr}}{4} [Z_{r+1}(q, t) + Z_{r-1}(q, t) + 2Z_r(q, t)], \quad (4)$$

with the initial condition  $Z_r(q, 0) = \exp(iqr)$ , and the boundary conditions  $Z_0(q, t) = 1$  and  $Z_L(q, t) = \exp(iqL(t + 1))$ . Equation (4) can be iterated  $t$  times, with the help of a computer, to obtain  $Z_1(q, t)$  explicitly [23]. See Figs. 1a and 1b for  $Z_1(q, t)$  at  $t = 10$  and  $500$ , respectively, for  $L = 16$ . We perform an inverse Fourier transform on  $Z_1(q, t)$  to obtain

$$p(m, t) = \frac{1}{2\pi} \int_{-\pi}^{\pi} Z_1(q, t) e^{iqm} dq. \quad (5)$$

This procedure leads to the exact distribution  $p(m, t)$  for any  $L$  and  $t$ .

Using the recursion relation (4), Takayasu et al. [10, 11] and Huber [12] obtained the probability distribution for  $L = \infty$ ,  $t = \infty$  to be  $p(m, t) \sim m^{-4/3}$ . We consider finite  $L$  and  $t$  and obtain exact results for  $p(m, t)$  using the procedure described above.

In a system of size  $L$ , there is a characteristic time  $t^* = L^2$  over which mass fluctuations spread diffusively across the system. For  $t \ll t^*$ , fluctuations spread across a length  $\mathcal{L}(t) = \sqrt{t} \ll L$ , whereas for  $t$  exceeding  $t^*$ , the system reaches a ‘steady state’ in a sense to be made precise below. Below, we discuss our results for  $p(m, t)$  separately for the two regimes: (a)  $t \ll t^*$  and (b)  $t \gg t^*$ . We restrict ourselves to relatively small values of  $L$ , namely,  $L = 8$  and  $16$ , as they suffice to show all the relevant features of  $p(m, t)$  and as going to higher values of  $L$  is computationally costly.

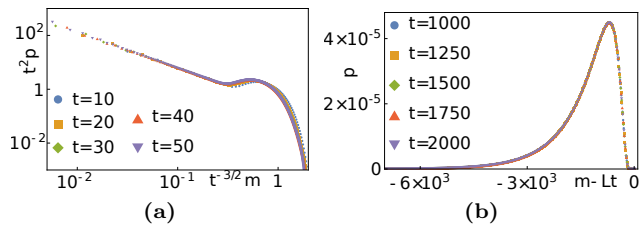
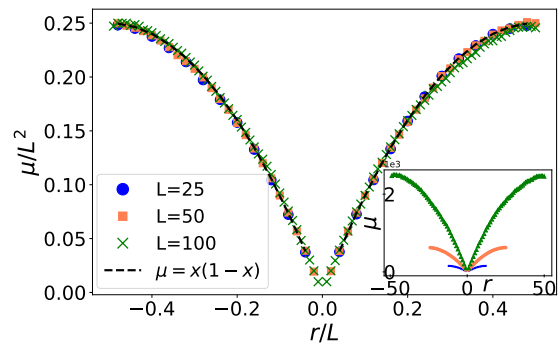


**FIG. 2.** (a): Scaling of  $p(m, t)$  in the regime  $t \ll t^*$ . (b): Scaling of the condensate peaks for  $t \gg t^*$ . The system size  $L = 16$ .

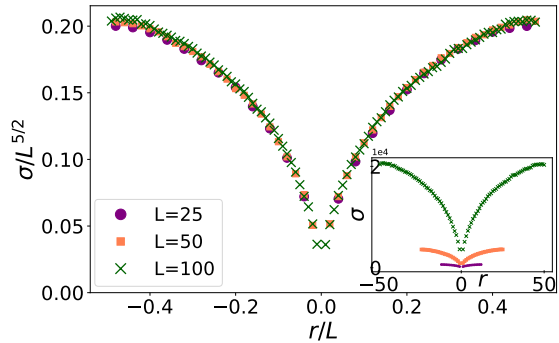
(a) To study  $p(m, t)$  in the regime  $t \ll t^*$ , we examine the cases  $t = 10$  and  $15$  for  $L = 8$  and  $16$  shown in Fig. 1c: the distribution is characterized by the power-law  $p(m) \sim m^{-4/3}$  followed by a hump. The hump corresponds to the presence of large condensates in the system, with typically one condensate in each region of length  $\mathcal{L}(t)$  [16]. The distribution is cut-off beyond the hump at  $m = (t + 1)L$ , which is the total mass in the system at time  $t$ . For different values of  $L$ , the distributions  $p(m, t)$  are identical except for the cut-off. For different values of  $t$ , on scaling  $m$  by  $t^{-3/2}$  and  $p(m, t)$  by  $t^2$ , for  $t \ll t^*$ , the curves collapse (see Fig. 2a), implying the scaling form  $p(m, t) \approx t^{-2} f(u)$ , where  $u = mt^{-3/2}$ . Note that the condensate hump is part of the scaling function. The region  $u < u_0 \simeq 0.6$  shows the aforementioned power-law decay, while the condensate hump appears for  $u > u_0$ , with  $f(u)$  decaying exponentially as  $u \rightarrow \infty$  [16].

(b) For a fixed  $t$  in the regime  $t \gg t^*$ , the distribution follows  $p(m, t) \sim m^{-4/3}$  for  $m \ll m^*$  and  $p(m) \sim \exp(-m/m^*)$  for  $m \gg m^*$ , where  $m^* = L^3 + L$  is a characteristic mass equal to the total mass in the system up to time  $t^*$ . Towards the end of this exponential tail the distribution exhibits a prominent peak, representing a single large condensate. The area under the peak is  $1/L$ , the probability to find the condensate at a randomly chosen site. In the steady state, the condensate peak in the distribution is seen to follow  $p(m, t) \approx H(m - Lt)$  (see Fig. 2b), showing that once  $t$  exceeds  $t^*$ , practically all the mass injected into the system is eventually absorbed by the condensate. Concomitantly, the mass distribution of the rest of the system, which corresponds to the portion before the condensate peak, assumes a time-independent form. Thus, we shall refer to the  $t \gg t^*$  regime as ‘steady state’, despite the fact that the condensate mass keeps growing.

We remark that the condensates did not appear in the treatments of [10–12], as they are missed in the limit  $t \rightarrow \infty$  in an infinite system. Our exact results for finite  $L$  and  $t$  show the existence of condensates and corroborates the conclusions of [16], which were based on numerical simulations. Condensates show up in both regimes of  $t$ , first as a hump (for  $t \ll t^*$ ) and then as a peak (for  $t \gg t^*$ ).



(a)



(b)

**FIG. 3.** (a) Scaling of  $\mu$  with  $L$ . (b) Scaling of  $\sigma$  with  $L$ . The plots are for  $L = 25, 50$  and  $100$ . The insets show the unscaled plots.

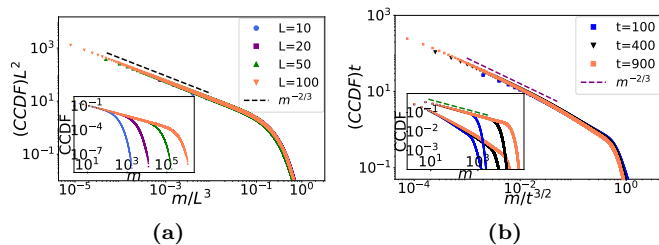
The condensate moves around the system accumulating mass, which raises intriguing questions about its impact on the surroundings. To address this, we perform numerical simulations and analyze the time-averaged mass profile *relative to the condensate*. We monitor the mean and standard deviation of the masses at position  $r$  with respect to the condensate in a system of size  $L$ . In other words, we shift the origin to the position of the condensate at each time step.

Figure 3a shows that in steady state, the mass profile across the full system is strongly affected by the moving condensate. The main plot depicts scaling of the mean mass  $\mu(r, L) = L^2 g_1(\frac{r}{L})$ . Our data is consistent with  $g_1(x) = x(1 - x)$ , a form that we establish analytically [23]. Similarly, in Fig. 3b, the main plot shows the scaling of the standard deviation  $\sigma(r, L) = L^{5/2} g_2(\frac{r}{L})$ . We observe that  $g_2(x) \sim x^{1/2}$  when  $x \ll 1$ .

The scaling forms for the mean and the standard deviation imply that for a given  $L$  the mass distribution  $P(m)$  varies with  $r$  and that it is a function of the scaled separation  $r/L$ . We observe that in the regime  $r/L \lesssim 1/2$ , the behavior of  $\mu$  and  $\sigma$  are consistent with the power-law

$$P(m) \sim m^{-\theta} \quad (6)$$

with  $\theta = 4/3$ . For a distribution of the form (6) with



**FIG. 4.** (a) Scaling of the CCDF for the masses on sites next to the condensate with  $L$  for  $L = 10, 20, 50,$  and,  $100$  at steady state. Inset: Unscaled plots. (b) Scaling of the CCDF for masses on the sites next to the condensate with  $t$  in the regime  $t \ll t^*$ . The inset shows CCDF vs  $m$  plotted at different times for masses on the sites next to the condensate and masses in the bulk along with the lines  $m^{-2/3}$  and  $m^{-1/3}$ , respectively.

$\theta < 2$ , we obtain the dependences  $\mu \sim L^{6-3\theta}$  and  $\sigma \sim L^{(9-3\theta)/2}$ . For  $\theta = 4/3$  this yields  $\mu \sim L^2$  and  $\sigma \sim L^{5/2}$ , matching the dependences obtained above from the scaling functions  $g_1$  and  $g_2$  for  $r/L \lesssim 1/2$ .

However, close to the condensate, where  $r/L \ll 1$ , the moments  $\mu$  and  $\sigma$  scale differently, with  $\mu \sim L$  and  $\sigma \sim L^2$ , implying a new value of power-law decay exponent  $\theta = 5/3$ . Thus, the value of the exponent changes from  $\theta = 4/3$  to  $\theta = 5/3$  as one transitions from the region far from the condensate  $r/L \sim 1/2$  to the region close to it ( $r/L \ll 1$ ), highlighting a distinct change of the mass distribution.

To check this directly, we monitor the mass distribution at sites next to the condensate by numerical simulations. We analyze the complementary cumulative distribution function  $\text{CCDF} \equiv \sum_{m'=1}^m P(m')$ . Here,  $m$  represents the mass on the site adjacent to the condensate. In Fig. 4a, the main plot shows the scaled CCDF plotted as  $\text{CCDF}L^2$  against  $m/L^3$ . We see that in steady state the  $\text{CCDF} \sim m^{1-\theta}$ , with  $\theta = 5/3$ .

The CCDF of masses relative to the condensate depicts a clear crossover as  $r/L$  varies, with the exponent  $\theta$  changing from  $4/3$  to  $5/3$  [23]. When  $r/L \ll 1$ , the  $\theta = 4/3$  region is small, and the  $\theta = 5/3$  region dominates. As  $r/L$  increases, the  $\theta = 4/3$  region continues to expand until it prevails everywhere.

These steady state results also have interesting implications for the regime  $t \ll t^*$ . As diffusive correlations in the system lead to the formation of subsystems of size  $\mathcal{L}(t)$ , this length scale effectively replaces the system size  $L$  in this regime. The main plot of Fig. 4b shows the CCDF of masses next to the condensate scaled using  $\mathcal{L}(t)$  in place of  $L$ . The inset in Fig. 4b shows the unscaled CCDFs in the bulk and adjacent to the condensate at different times, highlighting the presence of two distinct power law behaviors.

In fact, the two powers  $\theta = 4/3$  and  $5/3$  show up prominently even in a *single* configuration of a large system

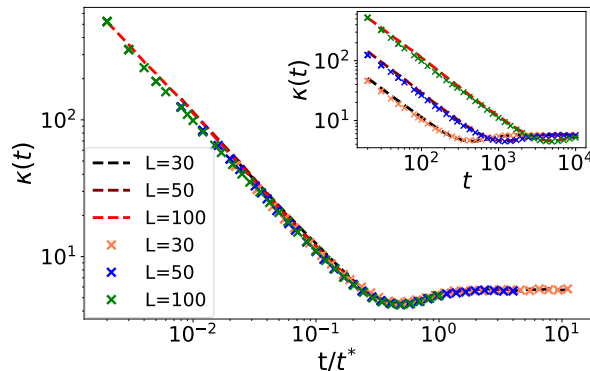


**FIG. 5.** Scaling collapse for  $\kappa(t)$  when plotted against  $t/t^*$  for  $L = 30, L = 50$  and,  $L = 100$ . The dashed lines and the crosses correspond to open and periodic boundary conditions, respectively. Inset: Unscaled plots.

for  $t \ll t^*$ . To demonstrate this, we simulated a system with  $L = 10^7$ . We identified the largest mass in each subsystem of length  $\mathcal{L}(t) = t^{1/2}$  as a condensate. The number of such subsystems  $N = L/\mathcal{L}(t)$ . Then, for each time we obtained frequency distributions: (1) for masses on the sites next to the condensates and (2) for masses across the full system, which we refer to as the bulk. We thereby found that the sites next to the condensates exhibit the mass distribution  $P(m) \sim m^{-5/3}$ . As time progresses, the size of each subsystem increases and  $N$  decreases. However, since the mass distribution around the condensate depends only on the ratio  $r/\mathcal{L}(t)$ , the region influenced by the condensate grows proportional to  $\mathcal{L}(t)$ . As a consequence, a *finite fraction* of the system is expected to display a different power law from that of the bulk due to the presence of condensates, even though the entire system remains translationally invariant.

Finally, we point out that in the steady state of Takayasu model with open boundary conditions, the exits of condensates with mass  $\sim O(L^3)$  [23], lead to large crashes of the total mass  $M(t)$  of the system in time. The crashes are followed by a build-up of  $M(t)$  due to input, followed again by crashes, and so on in an intermittent fashion, reminiscent of dragon king events [25, 26]. Intermittency, which signals breakdown of self-similarity, is quantified by the behavior of the structure functions  $S_n(t) = \langle [M(t) - M(0)]^n \rangle$  where  $\langle \dots \rangle$  denotes average over histories [27, 28]. A quantitative measure is provided by the flatness  $\kappa(t) = S_4(t)/S_2(t)^2$ , studied earlier in aggregation-fragmentation models with influx and outflux at the boundaries [28]. Intermittency is signalled by the divergence of  $\kappa$  in the limit  $t/t^* \rightarrow 0$  [27–29]. Figure 5 shows that  $\kappa \sim (t/t^*)^{-\phi}$  with  $\phi \simeq 0.9$ , implying strong intermittency in the system with open boundaries.

Interestingly, intermittency shows up even with periodic boundary conditions if we focus on  $M_{rest}(t)$ , the mass in the system excluding the condensate.  $M_{rest}(t)$

has fixed mean value in steady state, but shows intermittent fluctuations [23] with a divergent  $\kappa(t)$ , as the condensate acts as an absorbing boundary. This is clearly illustrated in Fig. 5.

In summary, we have identified a purely statistical mechanism for condensate formation. In the Takayasu model, our exact results for  $p(m, t)$  for finite  $L$  and  $t$  help to establish the presence of condensates, which lead to a hump in the distribution when  $t \ll t^*$ , and a sharp peak for  $t \gg t^*$ . In steady state, the movement of the single condensate reconfigures the mass profile on a macroscopic scale. An interesting and unexpected outcome is the occurrence of a new power law  $P(m) \sim m^{-5/3}$  in the region close to the condensate. Finally, successive build-ups and exits of the condensates from the Takayasu model with open boundaries lead to crashes of the total mass, characterized by strong intermittency.

In a broader vein, it would be interesting to look for strong imprints of condensates on the static and dynamic properties of other systems obeying aggregation-diffusion dynamics. On the theoretical end, the conserved mass aggregation model [18, 19] and the in-out model [30, 31] both exhibit condensates, and are therefore expected to share some of the signatures discussed above. Experimentally, biomolecular aggregates which are described within the Takayasu framework of aggregation and input [4–6], would be promising candidates to look for these signatures.

We thank Arghya Das and Himani Sachdeva for helpful discussions. M. B. acknowledges the support of the Indian National Science Academy (INSA). We acknowledge the support of the Department of Atomic Energy, Government of India, under Project Identification No. RTI4007.

---

[1] S. K. Friedlander and D. Smoke, *Haze: Fundamentals of aerosol dynamics* (Oxford University Press, New York, 2000).

[2] A. E. Scheidegger, *Hydrol. Sci. J.* **12**, 15 (1967).

[3] M. V. Smoluchowski, *Zeitschrift für Physik* **17**, 557 (1916).

[4] C. P. Brangwynne, T. J. Mitchison, and A. A. Hyman, *Proc. Natl. Acad. Sci. USA* **108**, 4334 (2011).

[5] J. Berry, C. P. Brangwynne, and M. Haataja, *Rep. Prog. Phys.* **81**, 046601 (2018).

[6] D. S. W. Lee, C.-H. Choi, D. W. Sanders, L. Beckers, J. A. Riback, C. P. Brangwynne, and N. S. Wingreen, *Nature Phys.* **19**, 586 (2023).

[7] G. Arsenadze, C. M. Caragine, T. Coakley, I. Eshghi, Y. Yang, A. Wofford, and A. Zidovska, *Biophys. J.* **123** (2024).

[8] H. Takayasu, I. Nishikawa, and H. Tasaki, *Phys. Rev. A* **37**, 3110 (1988).

[9] V. Privman, *Nonequilibrium statistical mechanics in one dimension* (Cambridge University Press, 1997).

[10] H. Takayasu, M. Takayasu, A. Provata, and G. Huber, *J. Stat. Phys.* **65**, 725 (1991).

[11] H. Takayasu, *Phys. Rev. Lett.* **63**, 2563 (1989).

[12] G. Huber, *Phys. A* **170**, 463 (1991).

[13] R. Rajesh and S. N. Majumdar, *Phys. Rev. E* **62**, 3186 (2000).

[14] T. M. Liggett, *Stochastic interacting systems: contact, voter and exclusion processes*, Vol. 324 (Springer Science & Business Media, 2013).

[15] S. N. Coppersmith, C.-h. Liu, S. Majumdar, O. Narayan, and T. A. Witten, *Phys. Rev. E* **53**, 4673 (1996).

[16] A. Das and M. Barma, *Indian J. Phys.* 10.1007/s12648-023-03030-1 (2023).

[17] M. R. Evans and T. Hanney, *J. Phys. A: Math. Gen.* **38**, R195 (2005).

[18] S. N. Majumdar, S. Krishnamurthy, and M. Barma, *Phys. Rev. Lett.* **81**, 3691 (1998).

[19] S. N. Majumdar, S. Krishnamurthy, and M. Barma, *J. Stat. Phys.* **99** (2000).

[20] C. Iyer, A. Das, and M. Barma, *Phys. Rev. E* **107**, 014122 (2023).

[21] D. A. Darling, *Trans. Am. Math. Soc.* **73**, 95 (1952).

[22] W. Feller, *An introduction to probability theory and its applications*, Vol. 2 (John Wiley & Sons, 1991).

[23] See Supplemental Material.

[24] A. J. Bray, *Adv. Phys.* **43**, 357 (1994).

[25] D. Sornette and G. Ouillon, *Eur. Phys. J. Special Topics* **205** (2012).

[26] G. Mikaberidze, A. Plaud, and R. M. D’Souza, *Phys. Rev. Res.* **5** (2023).

[27] U. Frisch, *Turbulence: the legacy of A. N. Kolmogorov* (Cambridge University Press, 1995).

[28] H. Sachdeva, M. Barma, and M. Rao, *Phys. Rev. Lett.* **110**, 150601 (2013).

[29] H. Sachdeva and M. Barma, *J. Stat. Phys.* **154**, 950 (2014).

[30] S. N. Majumdar, S. Krishnamurthy, and M. Barma, *Phys. Rev. E* **61**, 6337 (2000).

[31] R. Rajesh, *Phys. Rev. E* **69**, 036128 (2004).

# Supplemental Material: Condensates in aggregation processes with input: a new power law and intermittency

## THE MAXIMAL TERM IN A LÉVY DISTRIBUTION

Below we show that the largest of a number of terms drawn from a Lévy distribution has the attributes of a condensate. This continues to hold for the Takayasu model, despite correlations between variables.

Consider  $n$  random variables  $m_1, m_2, \dots, m_n$ . Suppose they are independent and identically distributed with the probability distribution function  $p(m) \sim m^{-(1+\alpha)}$  with  $\alpha < 1$ . Let  $S_n$  and  $M_n$  denote their sum and maximum respectively:  $S_n = \sum_{i=1}^n m_i$  and  $M_n = \max(m_1, m_2, \dots, m_n)$ . The variables  $S_n$  and  $M_n$  are strongly correlated and satisfy [1, 2]

$$\langle S_n/M_n \rangle \rightarrow \frac{1}{1-\alpha}, \quad (\text{S1})$$

This result indicates that the maximal term carries a finite fraction of the total mass, which is the hallmark of a condensate.

In the Takayasu model, the power-law decay part of the bulk probability distribution follows  $p(m) \sim m^{-4/3}$ , but the masses at different sites are not independent [3, 4] and hence (S1) is not expected to hold. We evaluated  $\langle S_n/M_n \rangle$  numerically for the Takayasu model at times  $t \ll t^*$  and found that  $\langle S_n/M_n \rangle \simeq 1.41$ , which is different from the value 1.5, which would result if we had independent variables with  $\alpha = 1/3$ . The fact that  $\langle S_n/M_n \rangle$  converges to a finite non-zero value indicates that the largest mass holds a significant fraction of the total mass.

## THE CHARACTERISTIC FUNCTION $Z_1(q)$

Here we discuss the manner in which the distribution  $p(m, t)$  is reflected in the corresponding characteristic function  $Z_1(q, t)$ . For  $t \ll t^* = L^2$  the distribution  $p(m, t)$  is characterized by a power-law decay followed by a hump with an exponential tail as in Fig. S1a. The power-law  $m^{-4/3}$ , is reflected by the cusp (see Figs. S1b and S1c) in  $Z_1(q, t)$ , which varies as  $q^{1/3}$ . The secondary maxima near the origin in the real and the imaginary parts of  $Z_1$ , shown in Figs. S1b and S1c for  $t = 6$  and 15 respectively, correspond to the condensate hump. As time increases from  $t = 6$  to 15, the condensate hump shifts to larger values of  $m$ , and the secondary maxima in  $Z_1(q, t)$  move closer to the origin.

Figures S1d and S1e show  $Z_1(q, t)$  after the steady state has been reached, at  $t = 150$  and 200 respectively, for  $L = 8$ . As before, the cusps here correspond to the power-law decay  $p(m) \sim m^{-4/3}$  (see Fig. S1a). The condensate part, which is a sharp peak in the large mass region, is reflected as rapid oscillations near the origin in  $Z_1(q, t)$ , reminiscent of the Fourier transform of a delta function  $\delta(m - m_c(t))$ , where  $m_c$  is the mass of the condensate. As time increases from  $t = 150$  to 200, the condensate mass  $m_c(t)$  increases, and the frequency of oscillations in  $Z_1(q, t)$  increases.

## ANALYTIC FORM FOR $\mu(r, L)$

Consider a system of size  $L$  with periodic boundary conditions following the Takayasu dynamics (see Eq.(1)). Let  $\mu(r, L)$  and  $J(r, L)$  denote the mean mass and the mean mass current, respectively, at position  $r$  with respect to the location of the condensate at steady state. As the masses follow symmetric diffusive dynamics, we write

$$J(r, L) = D[\mu(r, L) - \mu(r-1, L) - (\mu(r+1, L) - \mu(r, L))], \quad (\text{S2})$$

where  $D$  is the diffusion constant and the lattice spacing is 1. In the continuum limit this reduces to

$$J = -D\partial^2\mu/\partial r^2. \quad (\text{S3})$$

Evidently, at steady state,  $J(r, L)$  must satisfy the continuity equation

$$\partial J/\partial r = w, \quad (\text{S4})$$

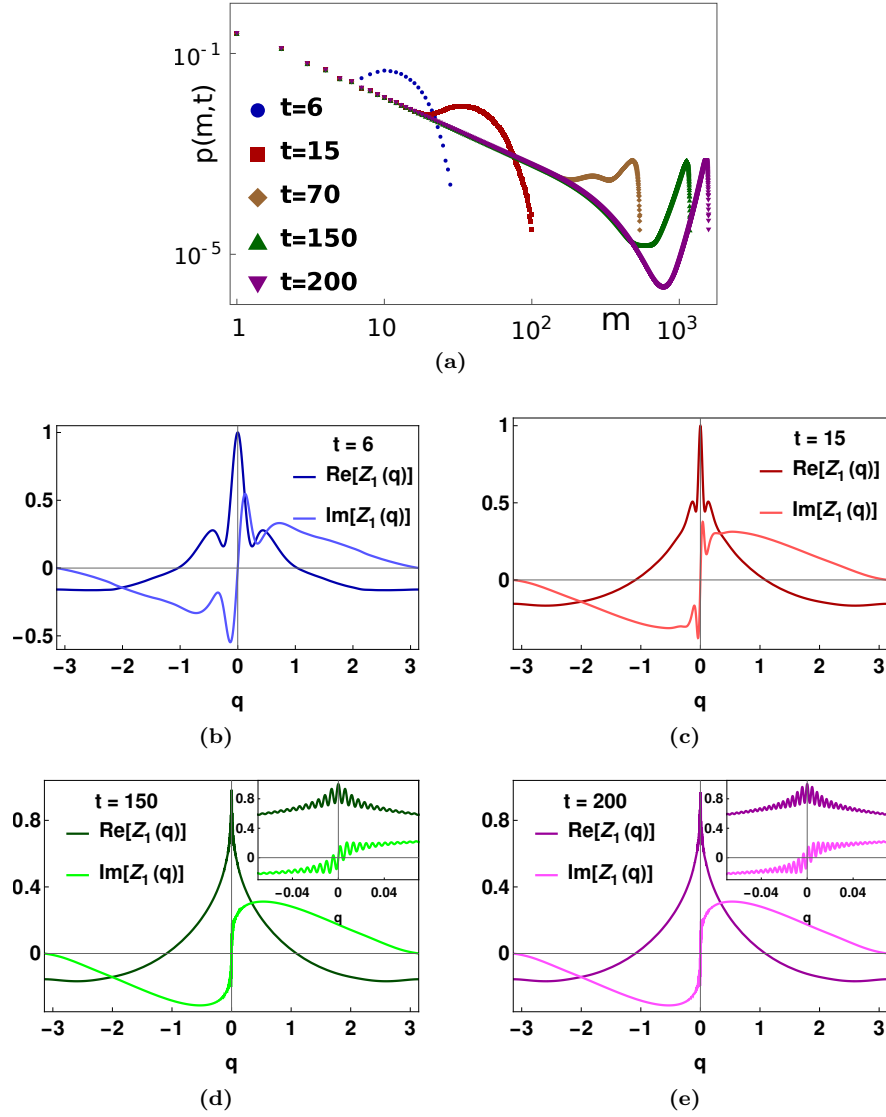


**FIG. S1.** The probability distribution  $p(m, t)$  and the corresponding Fourier transform  $Z_1(q)$  at different instants in the regimes  $t \ll t^*$  and  $t \gg t^*$  for  $L = 8$ . For  $t = 6$  and  $15 \ll t^*$ , the condensates lead to a hump in  $p(m, t)$  and correspond to secondary maxima near the origin in Fourier space. In steady state ( $t = 150$  and  $200$ ), the condensates appear as a peak (at the right edge) in  $p(m, t)$ , leading to rapid oscillations near the origin in  $Z_1(q)$ .

where  $w$  is the mass injected per unit length per unit time. Using Eqs. (S3), (S4), and the scaling form  $\mu(r, L) = L^2 g_1(x)$ , where  $x = r/L$ , we obtain the diffusion equation

$$D \frac{\partial^2 g_1}{\partial x^2} = -w, \quad (\text{S5})$$

with the boundary conditions  $g_1(0) = 0$  and  $g_1'(1/2) = 0$ . The former is obtained by considering the condensate as an absorbing boundary and the latter follows as  $\mu$  flattens as  $x \rightarrow 1/2$  corresponding to a local maximum. Equation (S5) is readily solved to obtain

$$g_1(x) = x(1 - x), \quad (\text{S6})$$

with  $w/2D = 1$  which matches the data.

## CROSSOVER OF POWER LAW IN THE CCDF FOR MASSES AROUND THE CONDENSATE

In Fig. S2 we show the scaled CCDF of masses around the condensate for various values of  $r/L$  for two system sizes,  $L = 50$  and  $L = 100$ . Notably, there is a distinct crossover in the  $m$ -dependence of  $P(m)$ , from  $\theta = 5/3$  to  $4/3$ , as  $r/L$  increases. When  $r/L \ll 1$ , the  $\theta = 5/3$  region is significant and the  $\theta = 4/3$  region is negligible. However, when  $r/L \lesssim 1/2$ , the  $\theta = 4/3$  region extends over the full range of  $m$ .

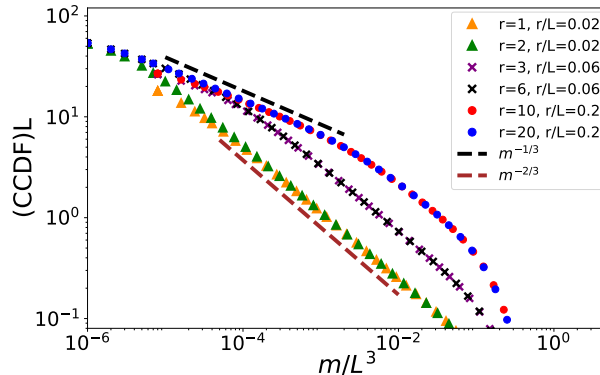


**FIG. S2.** The scaled plot of CCDF vs  $m$  for system sizes  $L = 50$  and  $L = 100$ . We see that  $\text{CCDF} \sim m^{1-\theta}$  with  $\theta = 5/3$  for  $r/L \ll 1$  and  $\theta = 4/3$  for  $r/L \lesssim 1/2$ , depicting a clear crossover.

## INTERMITTENCY

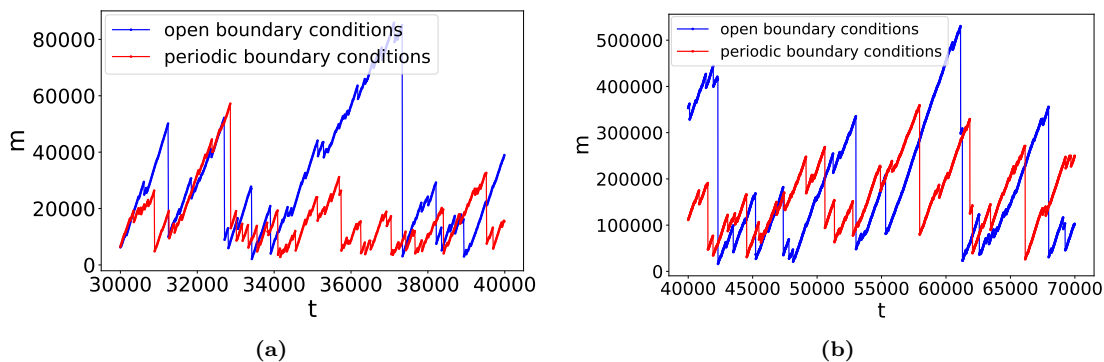


**FIG. S3.** (a) Plot of  $M(t)$  vs  $t$  for open boundary conditions (blue lines), and  $M_{rest}(t)$  vs  $t$  for periodic boundary conditions (red lines) for  $L = 50$  and for (b)  $L = 100$ .

In the Takayasu model, significant fluctuations are observed in the total mass  $M(t)$  with open boundary conditions. The fact that with periodic boundary conditions, the rest of the system (excluding the condensate) reaches a steady state, also leads to intermittency in  $M_{rest}(t)$ , as the condensate acts as an absorbing boundary. Figure S3 depicts the intermittent crashes and build-ups in  $M(t)$  and  $M_{rest}(t)$  with time.

To study intermittency, we need to analyze the flatness  $\kappa(t) = S_4(t)/S_2(t)^2$ , where  $S_n(t) = \langle [M(t) - M(0)]^n \rangle$ . For self-similar signals,  $S_n(t) \sim t^{\gamma n}$  as  $t/t^* \rightarrow 0$ , where  $\gamma$  is a constant. For intermittent signals, structure functions deviate from this form. We find that both  $S_2(t)$  and  $S_4(t) \sim t^\phi$  (see Fig. S4), and therefore  $\kappa \sim (t/t^*)^{-\phi}$  with  $\phi \simeq 0.9$  (see Fig. 5). This signals strong intermittency.

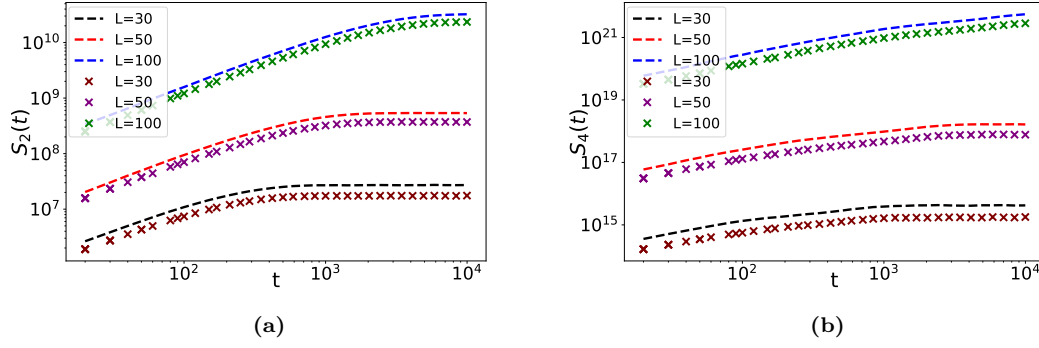


**FIG. S4.** Structure functions: (a)  $S_2(t)$  and (b)  $S_4(t)$  plotted against  $t$  for system sizes, namely,  $L = 30, 50$  and  $100$ . The dashed lines represent system with open boundary conditions and the crosses correspond to periodic boundary conditions.

- 
- [1] D. Darling, *Trans. Am. Math. Soc.* **73**, 95 (1952).  
 [2] W. Feller, *An introduction to probability theory and its applications*, Vol. 2 (John Wiley & Sons, 1991).  
 [3] R. Rajesh and S. N. Majumdar, *Phys. Rev. E: Stat. Phys., Plasmas, Fluids, Relat. Interdiscip. Top*, 3186 (2000).  
 [4] A. Das and M. Barma, *Indian J. Phys.* 10.1007/s12648-023-03030-1 (2023).